Please do not adjust margins **Polymer Chemistry**

Polymer Chemistry

Polyanhydride Nanoparticles by 'Click' Thiol-Ene Polymerization

Katie L. Poetz,[a,†] Olivia Z Durham[a,†] and Devon A. Shipp[*a,b]

The production of degradable polyanhydride-based nanoparticles using thiol-ene 'click' polymerizations is described. Linear polyanhydrides with number-average molecular weights of several thousand g/mol. were efficiently made through radical-mediated thiol-ene polymerization of 1,6-hexanethiol (HDT) and/or 3,5-dioxa-1,8-dithiooctane (EGDT), and 4-pentenoic anhydride (PNA). These linear polyanhydrides were used in the production of nanoparticles with diameters in the range of 250-400 nm using the emulsion-solvent evaporation method. The degradation of the particles were followed over 3-4 days, and show that hydrolysis of the anhydride moiety in the backbone occurs, decreasing the molecular weight of the polymer and reducing particle stability.

Introduction

Degradable polymer nanoparticles have become nouveau for many nano/bio-theranostic applications,[1-4] with degradability coming from common hydrolyzable functionalities such as esters, or from ortho ester, glycosidic, or disulphide bonds.[5] In particular, poly(lactic acid-*co*-glycolic acid) (PLGA) nanoparticles have been widely studied.[6, 7] Anhydrides are another well-known hydrolytically unstable moiety, yet are not anywhere near as commonly used in degradable polymers as esters in part because of the faster hydrolysis rates of anhydrides that may make them more difficult to work with and limits their shelf life.[8] In addition to this, synthesis of polyanhydrides has largely been limited to polycondensations, usually from diacids or diacyl anhydrides, either of which requires the removal of the condensate in order to achieve molecular weights even of a few thousand grams/mole. We improved this situation greatly by showing that polyanhydrides can simply and effectively be synthesized using thiol-ene 'click' polymerizations.[9-12] As part of the 'click' chemistry toolbox, these reactions can be initiated via photo, thermal, or redox means, are rapid and high yielding, and can provide easy post-polymerization functionalization.[13-15]

Here we show the utility of the thiol-ene 'click' polyanhydrides (PAs) for the production of degradable polymer nanoparticles. The entire lab-scale process can be achieved in as little as 45-60 minutes, even when it involves polymerization, polymer isolation, polymer dispersion and particle formation, and then

particle isolation. Scheme 1 illustrates the polymer synthesis and particle formation processes. Although polyanhydride-based particles in the micron- and sub-micron range have been shown to be effective in delivery of a number of therapeutics in the past,[2, 16-35] those nanoparticles were entirely based on polycondensation-derived polyanhydrides, thus requiring a far more laborious procedure to make the polymer before even attempting nanoparticle production. Our approach virtually eliminates this significant lead-time in polymer synthesis.
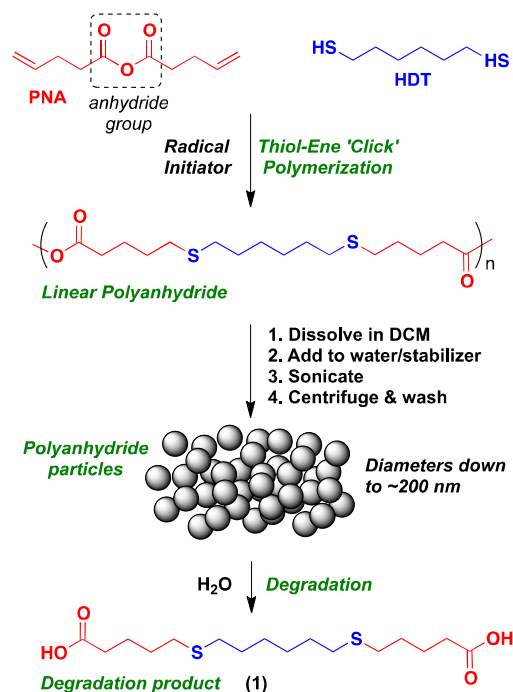
Scheme 1. Outline of polyanhydride synthesis using thiol-ene 'click' polymerization of 1,6-hexanethiol (HDT) and 4-pentenoic anhydride (PNA), and subsequent particle formation and degradation.

a. Department of Chemistry & Biomolecular Science, Clarkson University, Potsdam NY 13699-5810, U.S.A. Email: dshipp@clarkson.edu. Tel. +1-315-268-2393.
b. Center for Advanced Materials Processing, Clarkson University, Potsdam NY 13699-5810, U.S.A.
† These authors have contributed equally.

Experimental

Materials

The following materials were purchased from Sigma-Aldrich and were used as received after being characterized by ^{1}H NMR spectroscopy: 4-pentenoic anhydride (98%, PNA), 1,6-hexanedithiol (≥ 97%, HDT), 3,5-dioxa-1,8-dithiooctane (EGDT), 1-hydroxycyclohexyl phenyl ketone (99%), anhydrous dichloromethane (DCM), and polyvinyl alcohol (87-89% hydrolyzed PVA, 31-50K).

Instrumentation

^{1}H (400 MHz) nuclear magnetic resonance (NMR) spectroscopy was performed on Bruker Avance 400 with a BBO probe. The UV light source (365 nm) for polymer curing was an Oriel Instruments, model 68811, 500 W mercury xenon arc lamp (intensity ≈10 mW/cm^2. Gel permeation chromatography (GPC) was performed on a modular system comprised of the following: a Waters 515 high-pressure liquid chromatographic pump operating at 30°C, with tetrahydrofuran as the eluent, a Waters 717 autosampler, two Polymer Labs columns (PLgel Mixed C), and a Viscotek LR40 refractometer. Molecular weights were determined from polystyrene standards (Polymer Standards Service molecular weight range from 1270 to 1,230,000). Polymer particles were prepared by adding an aliquot of premade linear polymer dissolved in DCM to an aqueous phase and sonicating the reaction mixture using a Sonic Dismembrator Ultrasonic Processor (Model FB-120, 20 kHz, 120 W, 1/8" microtip (FB4422)) from Fisher Scientific. Polymer particles were analyzed using field emission scanning electron microscopy (FE-SEM) using a JEOL JSM 6300 instrument. For electron microscope analysis, product material was placed on an aluminum stub and dried in a vacuum oven until all solvent is removed. Prior to analysis, samples were sputter-coated with a thin Au/Pd layer. Particle size distributions were determined using dynamic light scattering (DLS) for aqueous dispersions using a ZetaPALS instrument (Brookhaven Instruments). This instrument was also used for the determination of zeta potential (ζ).

Polyanhydride synthesis

Polyanhydrides were typically synthesized by adding 0.5 mg (0.1 wt.%) 1-hydroxycyclohexyl phenyl ketone (photoinitiator) to a small vial, followed by anhydrous dichloromethane (0.46 mL, DCM), HDT (0.21 mL, 1.37 mmol.) and PNA (0.25 mL, 1.37 mmol.). The mixture was briefly stirred, and then placed under a mercury xenon arc lamp for 15 minutes. Other polymer compositions synthesized (PNA:EGDT and PNA:EGDT:HDT) were made using similar methods. The polymers were analyzed using gel permeation chromatography (GPC) and ^{1}H nuclear magnetic resonance (NMR) spectroscopy.

Polyanhydride nanoparticle synthesis

Most nanoparticle samples were prepared from linear PNA:HDT polymers unless otherwise stated. Each linear polymer was dissolved in DCM to yield a 50 mg/ml solution. A 1 ml aliquot of the polymer solution was then added to 4.5 ml water containing 0.25 wt.% PVA stabilizer, and then sonicated for 3 minutes while being submerged in an ice bath. The solution turned milky-white. The dispersion was then gently heated in a 60°C oil bath for 30 minutes to evaporate the DCM, and then centrifuged to isolate the particles.

Polyanhydride nanoparticle degradation

Polymer nanoparticles were prepared as described above and dispersed in either distilled water or PBS buffer. Degradations of the isolated polymer particles were performed by suspending the nanoparticles in 5 ml of either distilled water or PBS buffer. The resuspended particles were then degraded in an incubator shaker at 37°C. A 1 ml aliquot of the particle dispersion was taken at each time interval chosen for analysis. For GPC and NMR analysis, the nanoparticles were isolated by centrifugation and dissolved in THF (for GPC analysis) or CDCl$_3$ (for NMR analysis). For DLS and FE-SEM analysis, a few drops of the suspension were further diluted in the appropriate aqueous phase.

Results and discussion

Polyanhydride synthesis

Linear polyanhydrides, primarily based on equimolar amounts of 1,6-hexanethiol (HDT) and 4-pentenoic anhydride (PNA), were synthesized using photoinitiated thiol-ene 'click' chemistry. The molecular weights of these polyanhydrides typically ranged from several thousand up to ~15,000 g/mol. (relative to polystyrene standards) and because these polymers contain anhydride linkages in each repeat unit, they are easily hydrolyzed in the presence of water. As an example, when a linear 'click' polyanhydride with number average molecular weight (M_n) of 12,600 g/mol. and dispersity ($Đ$) of 2.23 was degraded in a mixture of THF and water (3/1 v/v), after 30 minutes the M_n was reduced to 2,200 g/mol. ($Đ$ = 2.42) and after 60 minutes the M_n was 1,300 g/mol. and $Đ$ = 2.03 (the GPC traces are shown in Figure SI-1 in the Supporting Information). Somewhat surprising is the approximately 1 hour timeframe this hydrolysis takes, even when the polymer is dissolved in a good solvent. This is an indication that the anhydride group within the polymer is not highly reactive, which is perhaps due to the hydrophobicity of the polymer. However, this observation also indicates that the dispersion of the polymer into an aqueous continuous phase during the preparation of particles should not lead to excessive hydrolysis and premature degradation of the polymer.

Polyanhydride nanoparticle synthesis

The polyanhydride particles were made using the emulsification-solvent evaporation procedures developed and widely utilized to make PLGA nanoparticles.[6, 36, 37] The polyanhydride (PA, M_n = 8,900 g/mol. in this example) was dissolved in DCM at the desired polymer concentration (50 mg/ml). This polymer solution (1 ml) was then added to water (4.5 ml) containing PVA (0.25 wt.%) as the stabilizer and then sonicated for 3 minutes on ice. The solution turned milky-

white during this process. Gentle heating of the dispersion at 60˚C for 30 minutes evaporated the DCM, and then particles were isolated via centrifugation.

Figure 1 shows FE-SEM images of polyanhydride particles (Fig. 1(a) and (b)) and the dynamic light scattering (DLS) curve (Fig. 1c)) from the same sample. The particles average around 330 nm in diameter based on the DLS data, and these numbers are corroborated by the FE-SEM images. Several repeats of this process yielded particle sizes that were within ~50 nm, thus indicating the reliability of the process. The particles in Figure 1 do not appear particularly smooth, but are mostly spherical. The sizes and approximate shapes are generally the same as PLGA-based polymer particles made via the emulsion-solvent evaporation method.[6, 36, 37]

The versatility of this method is illustrated by the production of several polymers with varying monomer composition, as described in Table 1, with EGDT, HDT and combinations of these two monomers as the source of dithiol. The resulting polymers were all capable of subsequently being able to be converted to nanoparticle form. This data indicates that nanoparticle diameters are not sensitive to polymer composition. However, Table 1 also shows that nanoparticle diameters are clearly dependent on polymer concentration, with diameters increasing as the concentration increases.

Table 1. Particle size (nm) determined by DLS for PA nanoparticle samples made using different monomers and different polymer concentrations in DCM.

Monomers[a,b]	Concentration (mg/ml)	Diameter (nm)
PNA:HDT	25	282
PNA:HDT	50	350
PNA:HDT	75	417
PNA:EGDT	25	265
PNA:EGDT	50	282
PNA:EGDT	75	318
PNA:HDT:EGDT	25	265
PNA:HDT:EGDT	50	287
PNA:HDT:EGDT	75	341

[a] Mole ratios used in polymerization: PNA:HDT = 1:1, PNA:EGDT = 1:1, and PNA:HDT:EGDT = 1:0.5:0.5.

[b] Molecular weights of polymers: PNA:HDT: M_n = 7,000 g/mol., Đ = 2.33 and M_n = 9,300 g/mol., Đ = 2.45 ; PNA:EGDT: M_n ~ 3,600 g/mol., Đ = 2.05; PNA:HDT:EGDT: M_n ~ 6,400 g/mol., Đ = 2.34.

Polyanhydride nanoparticle degradation

Degradation of the polyanhydride nanoparticles was studied by determining the size distribution by DLS over a few days. The nanoparticles (made with PA having M_n = 8,400 g/mol., Đ = 2.48) were made in two separate aqueous solutions (distilled water and PBS) and then degraded in these two solutions at 37°C. Figure 2 shows the GPC traces of the samples degraded in pure water as a function of time (GPC traces for the PA nanoparticles degraded in PBS are shown in Figure SI-2). The polymers were isolated at the specific time points by centrifugation and the dissolution into THF. It is clear that the molecular weight of the polymer decreases with time, due to the hydration of the anhydride linkages in the polymer backbone. Further evidence of this degradation mechanism is

seen in the peak at ~18 mL in the GPC traces, which is likely due to the degradation product (**1** in Scheme 1).

We note at this point that although PAs are well known to undergo surface erosion, a process in which the macroscopic PA object loses mass from the surface due to the confinement of hydrolytic degradation to the surface, in the case of nanoparticles we do not believe we will observe such an erosion mechanism. We have recently shown that crosslinked thiol-ene 'click' PAs exhibit surface erosion characteristics,[11, 12] but the objects studied were far larger than the nanoparticles examined here (mm vs. nm). This difference in size is important in terms of erosion mechanism because water penetration in many surface-eroding PAs, and hence hydrolysis depth, is often reported to be in the micron range.[38, 39] Hence, for large objects with dimensions mm and above the object appears to undergo surface erosion until the object size becomes commensurate to the water penetration depth. In terms of nanoparticles, the PA material is already smaller than the water penetration depth by a few orders of magnitude and so should exhibit bulk erosion characteristics.
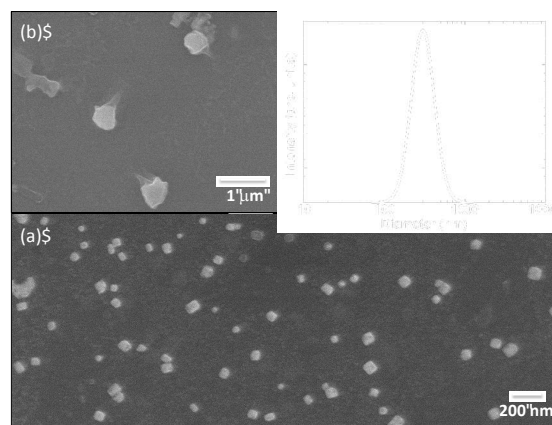

Figure 1. (a) FE-SEM images of PA (PNA:HDT) nanoparticles. (b) Higher-resolution FE-SEM image of PA nanoparticles. (c) DLS curves of PA nanoparticles. PA M_n = 8,900 g/mol.
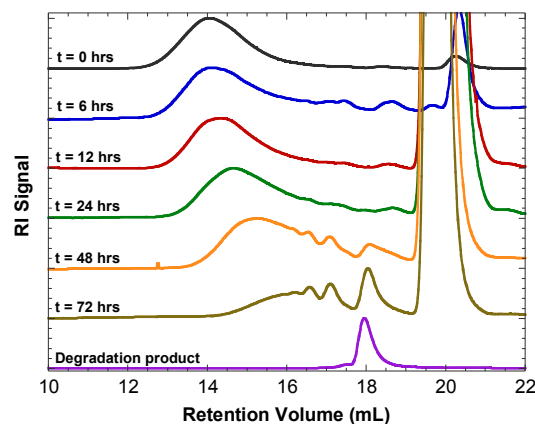

Figure 2. GPC traces of PA prepolymer (t=0 hrs, M_n = 8,400 g/mol., Đ = 2.48) and PA particles as a function of degradation time at 37°C in water. Also shown is the GPC trace of the model degradation product (**1** in Scheme 1).

^{1}H NMR spectra of the samples degraded in water and PBS solution (see Figures 3 and SI-3, respectively) indicate that the polymer indeed is undergoing hydrolysis at the anhydride group. In particular, the appearance of a peak at ~2.4 ppm, indicative of the α-proton of the carboxylic acid produced after hydrolysis, throughout the degradation process underscores this conclusion. Integration of the peak at ~2.4 ppm and comparison of the integrals to the peaks due to the non-degrading segment polymer backbone (peak at ~1.4 ppm) allowed for degradation kinetics to be determined. First-order plots were constructed (Figure SI-4) but were non-linear, particularly for the PBS solution experiment. We believe the non-linearity of these first-order plots to be due to the aggregation behaviour of the nanoparticles, which is more pronounced in PBS than in water (*vide infra*).
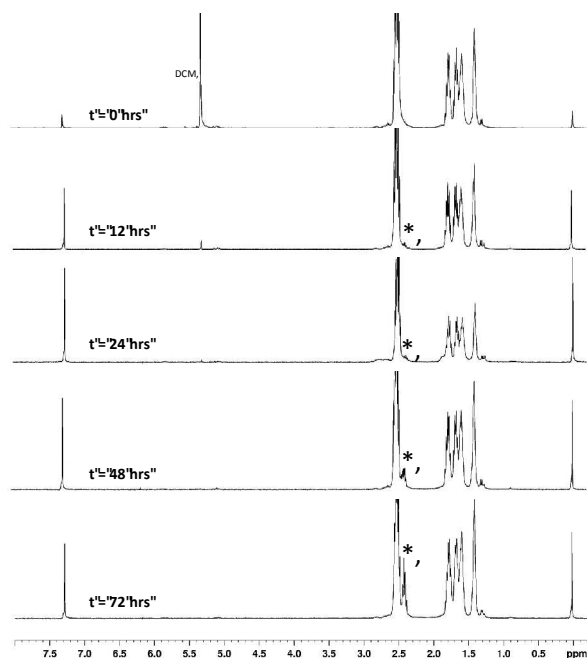

Figure 3. ^{1}H NMR spectra (CDCl$_3$) of PA particles as a function of degradation time in water at 37°C. Peak at ~2.4 ppm due the proton a to the carboxylic acid is indicated by the asterisks.

Average particle diameters determined by DLS of these same samples presented in Table 2 also confirm that large changes occur over the 72 hours the sample was dispersed in water and PBS solution (DLS curves can be found in Figure SI-5, Supporting Information). In water, the average particle size increased slightly in the first 48 hours, but then dramatically after 48 hours, indicating significant aggregation. A similar trend is seen in the DLS data from particles made from the same polymer but dispersed in PBS solution, although aggregation occurs slightly earlier, after 24 hours. Zeta potential measurements in water or PBS solution indicated that the particles have essentially no charge over the 72 hour degradation period, indicating that even though the hydrolysis process is producing carboxylic acids end groups, a negative charge does not build on the surface, as one might expect.

Since no surface charge is accumulated, the particles do not gain any stabilization through electrostatic forces. Analysis of SEM images (using a different PA nanoparticle sample; M_n = 7,000 g/mol., Đ = 2.33) also indicates that aggregation occurs (Figure 4) at longer times. In this case, it appears that a slightly lower molecular weight PA led to earlier aggregation, after 12 hours. Of course, the aggregation seen in these images may be a result of sample preparation for SEM analysis. Although Lee and Chu[35] observed similar aggregation in their study of the degradation of nanoparticles based on polyanhydride made from sebacic acid (SA) and 1,3-bis(*p*-carboxyphenoxy)propane (CPP), the most commonly studied polyanhydride in either bulk or particle forms, there are few reports regarding polyanhydride nanoparticle stability during degradation.

Table 2. Particle size (nm) determined by DLS for PA nanoparticle samples suspended in water at 37$^{\text{o}}$C (M_n ~ 8,400 g/mol., Đ = 2.48).

Time (hr)	Particle Size (nm)	
	In water	In PBS solution
0	336	356
6	339	385
12	351	332
24	362	340
48	380	~8800
72	~3700	~1800

The aggregation behaviour is clearly related to the degradation process, and is most likely a result of the generation of oligomers and small molecules (such as the degradation product **1**, depicted in Scheme 1) that decreases the ability of the PVA to provide steric stabilization[40] of the nanoparticles. This destabilization may be due to an increase in depletion forces,[41, 42] where the newly generated degradation products act as the depletants. The PVA might also graft to the particles via nucleophilic acyl addition to the anhydride group, thereby affecting stabilization; grafting of PVA has even been shown to occur and be important in radical emulsion polymerizations of acrylics.[43, 44] Another cause may be due to changes in nanoparticle surface charge, which would result from the generation of carboxylates during the hydrolysis of the anhydride groups. This could potentially alter the stabilization mechanism of the nanoparticles, which are largely sterically stabilized and carry very little charge prior to degradation (zeta potential measurements indicate that the nanoparticles carry essentially no charge at pH 7.1). Further studies into the stabilization/destabilization mechanism are currently being carried out.

Conclusion

In conclusion, we have shown that linear thiol-ene 'click' polyanhydrides, which can be easily synthesized within minutes, can then be used to make polyanhydride nanoparticles dispersed in aqueous media. The nanoparticles have diameters from a few hundred nanometers. The nanoparticles are shown to degrade over the course of a day or two, depending on the conditions to which they are

exposed. The degradation process causes aggregation of the nanoparticles. The ease and simplicity by which these particles can be made, along with their latent functionality that potentially allows a variety of conjugation chemistries to be activated, augurs well for their potential use in a host of biomedical applications, in particular drug delivery. We will report on such applications in the near future.

Acknowledgements

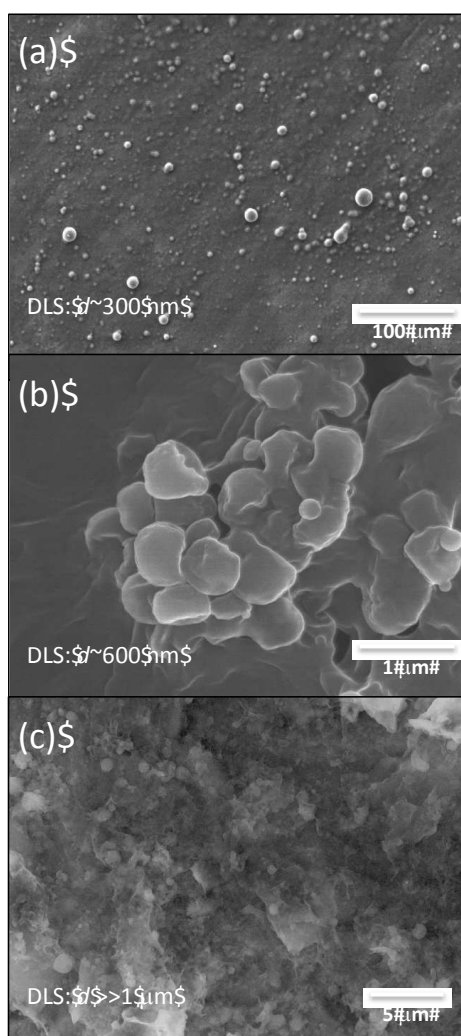**Figure 4.** FE-SEM images of PA (PNA:HDT) nanoparticles (M_n ~ 7,000 g/mol., Đ = 2.33) degraded in water at 37°C after various times. (a) 0 hrs. (b) 12 hrs. (c) 24 hrs. Diameters (*d*) determined by DLS are given on each image.

References

1   A. L. Sisson, M. Schroeter and A. Lendlein, in *Handbook of Biodegradable Polymers: Synthesis, Characterization and Applications*, ed. A. Lendlein, Sisson, A., Wiley-VCH Verlag, Weinheim, Germany, 2011, pp. 1-21.

2   F. Jia, X. P. Liu, L. H. Li, S. Mallapragada, B. Narasimhan and Q. Wang, *J. Control. Release*, 2013, **172**, 1020-1034.

3   M. A. Phillips, M. L. Gran and N. A. Peppas, *Nano Today*, 2010, **5**, 143-159.

4   G. Vilar, J. Tulla-Puche and F. Albericio, *Curr. Drug Deliv.*, 2012, **9**, 367-394.

5   A. Lendlein and A. Sisson, eds., *Handbook of Biodegradable Polymers: Synthesis, Characterization and Applications*, Wiley-VCH Verlag, Weinheim, Germany, 2011.

6   S. Acharya and S. K. Sahoo, *Adv. Drug Deliv. Rev.*, 2011, **63**, 170-183.

7   J. Panyam and V. Labhasetwar, *Adv. Drug Deliv. Rev.*, 2003, **55**, 329-347.

8   A. Domb, J. P. Jain and N. Kumar, in *Handbook of Biodegradable Polymers: Synthesis, Characterization and Applications*, eds. A. Lendlein and A. Sisson, 2011, pp. 45-75.

9   D. A. Shipp, C. W. McQuinn, B. G. Rutherglen and R. A. McBath, *Chem. Commun.*, 2009, 6415-6417.

10 B. G. Rutherglen, R. A. McBath, Y. L. Huang and D. A. Shipp, *Macromolecules*, 2010, **43**, 10297-10303.

11 K. L. Poetz, H. S. Mohammed, B. L. Snyder, G. Liddil, D. S. K. Samways and D. A. Shipp, *Biomacromolecules*, 2014, **15**, 2573-2582.

12 K. L. Poetz, H. S. Mohammed and D. A. Shipp, *Biomacromolecules*, 2015, **16**, 1650-1659.

13 C. E. Hoyle, T. Y. Lee and T. Roper, *J. Polym. Sci. Part A: Polym. Chem.*, 2004, **42**, 5301-5338.

14 C. E. Hoyle and C. N. Bowman, *Angew. Chem. Int. Ed.*, 2010, **49**, 1540-1573.

15 B. S. Sumerlin and A. P. Vogt, *Macromolecules*, 2010, **43**, 1-13.

16 E. Mathiowitz and R. Langer, *J. Control. Release*, 1987, **5**, 13-22.

17 E. Mathiowitz, W. M. Saltzman, A. Domb, P. Dor and R. Langer, *J. Appl. Polym. Sci.*, 1988, **35**, 755-754.

18 E. Mathiowitz, J. S. Jacob, Y. S. Jong, G. P. Carino, D. E. Chickering, P. Chaturvedi, C. A. Santos, K. Vijayaraghavan, S. Montgomery, M. Bassett and C. Morrell, *Nature*, 1997, **386**, 410-414.

19 C. G. Thanos, Z. Liu, J. Reineke, E. Edwards and E. Mathiowitz, *Pharm. Res.*, 2003, **20**, 1093-1100.

20 A. P. Morello, N. Forbes and E. Mathiowitz, *J. Microencapsul.*, 2007, **24**, 40-56.

21 S. Furtado, D. Abramson, R. Burrill, G. Olivier, C. Gourd, E. Bubbers and E. Mathiowitz, *Int. J. Pharm.*, 2008, **347**, 149-155.

22 C. Berkland, M. J. Kipper, B. Narasimhan, K. K. Kim and D. W. Pack, *J. Control. Release*, 2004, **94**, 129-141.

23 B. Carrillo-Conde, A. Garza, J. Anderegg and B. Narasimhan, *J. Biomed. Mater. Res. Part A*, 2010, **95A**, 40-48.

24 L. K. Petersen, C. K. Sackett and B. Narasimhan, *Acta Biomater.*, 2010, **6**, 3873-3881.

25 B. Carrillo-Conde, E. H. Song, A. Chavez-Santoscoy, Y. Phanse, A. E. Ramer-Tait, N. L. B. Pohl, M. J. Wannemuehler, B. H. Bellaire and B. Narasimhan, *Mol. Pharm.*, 2011, **8**, 1877-1886.

26 L. K. Petersen, A. S. Determan, C. Westgate, L. Bendickson, M. Nilsen-Hamilton and B. Narasimhan, *J. Biomater. Sci.-Polym. Ed.*, 2011, **22**, 1237-1252.

27   L. K. Petersen, A. E. Ramer-Tait, S. R. Broderick, C. S. Kong, B. D. Ulery, K. Rajan, M. J. Wannemuehler and B. Narasimhan, *Biomaterials*, 2011, **32**, 6815-6822.

28   C. K. Sackett and B. Narasimhan, *Int. J. Pharm.*, 2011, **418**, 104-114.

29   M. P. Torres, J. H. Wilson-Welder, S. K. Lopac, Y. Phanse, B. Carrillo-Conde, A. E. Ramer-Tait, B. H. Bellaire, M. J. Wannemuehler and B. Narasimhan, *Acta Biomater.*, 2011, **7**, 2857-2864.

30   A. V. Chavez-Santoscoy, R. Roychoudhury, N. L. B. Pohl, M. J. Wannemuehler, B. Narasimhan and A. E. Ramer-Tait, *Biomaterials*, 2012, **33**, 4762-4772.

31   L. Huntimer, A. E. Ramer-Tait, L. K. Petersen, K. A. Ross, K. A. Walz, C. Wang, J. Hostetter, B. Narasimhan and M. J. Wannemuehler, *Adv. Healthc. Mater.*, 2013, **2**, 369-378.

32   V. B. Joshi, S. M. Geary, B. R. Carrillo-Conde, B. Narasimhan and A. K. Salem, *Acta Biomater.*, 2013, **9**, 5583-5589.

33   S. L. Haughney, K. A. Ross, P. M. Boggiatto, M. J. Wannemuehler and B. Narasimhan, *Nanoscale*, 2014, **6**, 13770-13778.

34   K. A. Ross, H. Loyd, W. W. Wu, L. Huntimer, M. J. Wannemuehler, S. Carpenter and B. Narasimhan, *J. Biomed. Mater. Res. Part A*, 2014, **102**, 4161-4168.

35   W.-C. Lee and I.-M. Chu, *J. Biomed. Mater. Res. Part B: Appl. Biomater.*, 2008, **84B**, 138-146.

36   F. Danhier, E. Ansorena, J. M. Silva, R. Coco, A. LeBreton and V. Préat, *J. Control. Release*, 2012, **161**, 505-522.

37   J. V. Natarajan, C. Nugraha, X. W. Ng and S. Venkatraman, *J. Control. Release*, 2014, **193**, 122-138.

38   A. Göpferich and J. Tessmar, *Adv. Drug Deliv. Rev.*, 2002, **54**, 911-931.

39   F. vonBurkersroda, L. Scheld and A. Göpferich, *Biomaterials*, 2002, **23**, 4221-4231.

40   C. A. Finch, *Polyvinyl Alcohol: Properties and Applications*, Wiley, New York, 1973.

41   Y. Mao, M. E. Cates and H. N. W. Lekkerker, *Physica A*, 1995, **222**, 10-24.

42   S. Ji and J. Y. Walz, *Curr. Opin. Colloid Interface Sci.*, 2015, **20**, 39-45.

43   T. Okaya, A. Suzuki and K. Kikuchi, *Colloids Surf.*, 1999, **A153**, 123-125.

44   K. Yuki, M. Nakameae, T. Sato, H. Murayama and T. Okaya, *Polym. Int.*, 2000, **49**, 1629-1635.